Study of T_1- and T_2-Relaxation by Microwave Pulse Techniques: Rotational Transition $J=0-1$ of HCCF, J-Dependence of Rotational Transitions of SO_2, and l-Type Doublet Transitions of $HC^{15}N$ Perturbed by Self, H_2, D_2, and He

S. C. Mehrotra* and H. Mäder

Abteilung Chemische Physik im Institut für Physikalische Chemie der Universität Kiel

Z. Naturforsch. **43a**, 454–468 (1988); received February 23, 1988

With a K-band bridge type superhet spectrometer, the pressure dependence of the population decay rate $1/T_1$ by using a $(\pi, \tau, \pi/2)$ pulse technique, and of the coherence decay rate $1/T_2$ by using a $\pi/2$-pulse technique, have been determined for the following systems at room temperature: (a) rotational transition $J=0-1$ of fluoroacetylene (HCCF), (b) seven rotational transitions of sulfur dioxide (SO_2) with $5 \leqq J \leqq 37$, both (a) and (b) with pure gases, and (c) l-type doublet transitions of hydrogen cyanide ($HC^{15}N$) in the (01^10) vibrational state with $J=9$ and 10 using $HC^{15}N$, H_2, D_2 and He as perturbers. A theoretical treatment of Bloch-type equations with a special attention to the M-degeneracy of the energy levels is also considered to describe the microwave pulse experiments. For systems (b) and (c), the values of $1/T_1$ are found to be significantly smaller than corresponding values of $1/T_2$, indicating adiabatic collisions as a dominant mechanism for the decay of sample coherence. For the system (a), the value of $1/T_1$ is found to be slightly greater than the corresponding value of $1/T_2$. The normalized perturbative collision theory proposed earlier has been applied to explain the results of systems (a) and (c). The unsatisfactory agreement between theory and experiment for the system (c) indicates that a nonperturbative approach or a higher order perturbation treatment should be taken into consideration for a better description of collision dynamics.

I. Introduction

The relaxation time T_1 describes the relaxation of the population difference between two energy levels, whereas the relaxation time T_2 describes the relaxation of sample polarization associated with two levels of a transition under consideration. These relaxation times contain different information about collisions. A collision may be classified into one of the following types depending on its effect on T_1 and T_2:

(i) Adiabatic collisions which change only the phase of the wavefunctions of colliding molecules or the spatial orientation of the angular momentum without a transfer of energy, contribute only to $1/T_2$.

(ii) Collisions which induce transitions between the energy levels under consideration contribute approximately twice as effective to $1/T_1$ than to $1/T_2$.

(iii) Inelastic collisions other than type (ii) contribute similarly to $1/T_1$ and $1/T_2$.

There are very few systems for which both values of $1/T_1$ and $1/T_2$ have been investigated in gas phase [1, 2]. For most systems studied so far it has been found that the value of $1/T_1$ is equal to the corresponding value of $1/T_2$ within the experimental uncertainties. This indicates that collisions of type (iii) are dominant in gas phase. In case of the NH_3 system it has been found that the values of T_1/T_2 lie between 1 and 2 for different inversion lines [3–5]. This behaviour is due to the fact that collisions of type (ii) are also important, besides collisions of type (iii), as has been successfully explained using a perturbative approach to collision dynamics [5–7]. For some systems the values of $1/T_1$ have been reported to be slightly smaller than the corresponding values of $1/T_2$ [8]. However, there was no system known previous to this work for which the value of $1/T_1$ is considerably smaller than the corresponding value of $1/T_2$.

Collisions of type (i) are generally believed to be weak collisions, i.e. collisions for which the intermolecular interaction energy is small with respect to the spacing of rotational energy levels. On the contrary, strong collisions are assumed to be inelastic collisions with transition probabilities to many rota-

* Permanent address: Department of Physics. Marathwada University, Aurangabad 431002, India.

Reprint requests to Prof. Dr. H. Mäder, Abteilung Chemische Physik im Institut für Physikalische Chemie der Universität Kiel, Olshausenstr. 40–60, D-2300 Kiel, FRG.

0932-0784 / 88 / 0500-0454 $ 01.30/0. – Please order a reprint rather than making your own copy.

Dieses Werk wurde im Jahr 2013 vom Verlag Zeitschrift für Naturforschung in Zusammenarbeit mit der Max-Planck-Gesellschaft zur Förderung der Wissenschaften e.V. digitalisiert und unter folgender Lizenz veröffentlicht: Creative Commons Namensnennung-Keine Bearbeitung 3.0 Deutschland Lizenz.

This work has been digitalized and published in 2013 by Verlag Zeitschrift für Naturforschung in cooperation with the Max Planck Society for the Advancement of Science under a Creative Commons Attribution-NoDerivs 3.0 Germany License.

Zum 01.01.2015 ist eine Anpassung der Lizenzbedingungen (Entfall der Creative Commons Lizenzbedingung „Keine Bearbeitung") beabsichtigt, um eine Nachnutzung auch im Rahmen zukünftiger wissenschaftlicher Nutzungsformen zu ermöglichen.

On 01.01.2015 it is planned to change the License Conditions (the removal of the Creative Commons License condition "no derivative works"). This is to allow reuse in the area of future scientific usage.

tional levels, since the translational energy at room temperature is very large with respect to the rotational energy differences. However, a strong collision may also be of type (i). This type of collisions was described first using a nonperturbative approach to collision dynamics [9]. A first order perturbative treatment is likely to underestimate the influence of adiabatic collisions. For example, in case of linear molecules such theoretical procedure results in collision-induced transitions of type (ii) and (iii) if only dipolar interaction is considered. Second order dipole-type collisional transitions would contribute to collisions of type (i), which will make the value of $1/T_1$ smaller than the corresponding value of $1/T_2$. Inadequacies of previous first order perturbative approaches to binary collision theory have also been found during recent investigations on the pressure dependence of $1/T_2$-rates for various l-type doublet transitions of $HC^{15}N$, exhibiting significant differences between theoretical and experimental results [10].

The objective of the present paper is to report investigations of the pressure dependence of $1/T_1$ and $1/T_2$ for K-band transitions of HCCF, SO_2, and $HC^{15}N$. In the next section, the experimental procedures are described. In Sect. III, Bloch-type equations for two M-degenerate levels are considered to understand the performed pulse experiments.

A perturbative theory has also been used to compute the values of $1/T_1$ and $1/T_2$ for HCCF and $HC^{15}N$ with consideration of long range interactions. The experimental and theoretical results are given in Section IV. The conclusions of the paper are summarized in the last section.

II. Experimental

A K-band bridge type superhet spectrometer was used for the measurements of T_1- and T_2-relaxation times. The details of the spectrometer are given in an earlier paper [11]. The relaxation time T_1 was determined by the "$\pi, \tau, \pi/2$"-pulse sequence method as described recently [12]. The power of the pulsed microwave radiation was chosen to be about 100 mW in each arm of the bridge for system (a), and about 250 mW for systems (b) and (c). The relaxation time T_2 was determined with analysis of the transient emission signal following a single pulse excitation [11]. The experimental procedure is briefly described in the following.

Before filling the sample gas into absorption cell, the bridge was adjusted for carrier suppression to achieve rejection of the microwave pulses. At a given sample pressure, the pulse sequence experiment for analysis of T_1-relaxation was performed first according to the procedure given in [12]. Then, at the same pressure, the second pulse of the sequence was removed and the first pulse was adjusted in length to result in maximum transient emission signal after the end of the pulse ("effective $\pi/2$-pulse"). With change of the delay between the end of the first pulse and the gate of the Boxcar integrator the averaged transient emission signal was then probed to obtain information about T_2-relaxation. Thus, the experiments for determination of $1/T_1$- and $1/T_2$-rates could be performed at different pressures one after the other, thereby eliminating systematic errors from pressure uncertainties.

When performing the pulse sequence experiments, it has been observed that for the maximum microwave power available in our experiments, the length of the first pulse could not be adjusted for all investigated systems to yield no observable signal during the delay period between the pulses. Such "effective π-pulses" could readily be achieved for the transition $J=0-1$ of HCCF but not for the studied transitions of SO_2 and $HC^{15}N$. For the latter systems, a residual sample polarization after the end of the pulse was observed irrespective of the pulse length which was then adjusted to approximately twice the length of an "effective $\pi/2$-pulse" resulting in minimum emission signal during the delay period.

As shown in the next section, the observed signal in the pulse sequence experiment for determination of T_1 can generally be described by the expression

$$S(t) = \sum_{\substack{K \geqq 0 \\ \text{(even)}}} A_K \exp[-t/T_1(K)] + \sum_{\substack{K \geqq 1 \\ \text{(odd)}}} B_K \exp[-t/T_2(K) - t^2/4q^2] + C, \quad (1)$$

where A_K, B_K, C are constants and the range of K-values in the two sums depends on the J-values of the considered transition. $T_1(K)$ and $T_2(K)$ are relaxation parameters defined in the next section, and $q = \sqrt{\ln 2}/2\pi\ \Delta\nu_D$, with $\Delta\nu_D$ the Doppler half width. However, if one attempts to use more than one exponential term in (1) as a fitting expression for the observed signal, a very high correlation between the fitting parameters, i.e. A_K, B_K, C, $1/T_1(K)$ and $1/T_2(K)$,

has been obtained. Therefore "effective" values for $1/T_1$ were determined by neglecting the second sum in (1) (i.e. assuming $B_K = 0$ for all K) and taking only one exponential term in the first sum, setting $A_K = 0$ for $K \neq 0$ or assuming all relaxation parameters $T_1(K)$ to be identical.

The value of $1/T_2$ was obtained by fitting the observed signal of the transient emission experiment according to the expression

$$S(t) = B \exp[-t/T_2 - t^2/4q^2] + C \tag{2}$$

with B, $1/T_2$ and C as fitting parameters, where q was kept fixed and calculated from the Doppler half width of the investigated transitions.

From the fit results for $1/T_1$ and $1/T_2$ at different sample pressures, the coefficients for the linear pressure dependence were then evaluated by using a linear least squares fit, weighting the $1/T_1$ and $1/T_2$ data points with their standard deviations in the expressions

$$1/T_1 = \alpha_1 + \beta_1 p, \tag{3a}$$

$$1/T_2 = \alpha_2 + \beta_2 p, \tag{3b}$$

respectively. For the pure gases, p is the total sample pressure and the intercepts α_1 and α_2 are primarily due to wall collisions. In case of the mixtures of $HC^{15}N$ with H_2, D_2 and He, the contribution to $1/T_1$ and $1/T_2$ from self-collisions of $HC^{15}N$ at a fixed partial pressure was subtracted from the experimentally determined $1/T_1$- or $1/T_2$-values and (3 a, b) were used for the analysis with p being the partial pressure for H_2, D_2 and He.

SO_2 (purity 99.98%) was purchased from J. T. Baker Co. and used without further purification. $HC^{15}N$ (purity about 99%) was prepared from $KC^{15}N$, purchased from MSD Sharp-Dome Co. with 95% isotopic abundance. Fluoroacetylene was obtained with a purity of about 97% (having some impurities of acetylene) by dehalogenation of E-1-bromo-2-chloro-2-fluoro-ethylene with Mg in tetrahydrofurane, using a similar method as given by Viehe et al. [13]. Pressure measurements were made using an MKS Baratron 310 B capacitance manometer. A 20 l bulb was attached to the vacuum system in order to stabilize the pressure. The pressure ranges for the pure gases were 1 mTorr to 5 mTorr for $HC^{15}N$ and SO_2, and 1 mTorr to 20 mTorr for HCCF. For the mixtures of $HC^{15}N$ with H_2, D_2 and He the partial pressures for the foreign gases were in the range from 1 mTorr to 20 mTorr at a fixed partial pressure of $HC^{15}N$ of about 2 mTorr. All measurements were done at room temperature.

III. Theory

The general theory of microwave transient phenomena has been discussed extensively in the literature [14, 15]. However, little attention has been given to the effects of energy level degeneracies on the observed molecular signals. The objective of this section is to include the spatial M-degeneracy of rotational levels in the theoretical description of "$\pi/2$"- and "π, τ, $\pi/2$"-pulse experiments. It will be shown in particular that "effective π-pulses" may not be achieved for transitions between levels with high M-degeneracy. As pointed out in the previous section, such behaviour has been observed for l-type doublet transitions of $HC^{15}N$ and rotational transitions of SO_2.

The theory to analyze the pulse experiments described above is briefly outlined here, following closely previous formulations [8, 9]. The considered energy states are specified by the quantum numbers J and M for the rotational angular momentum and its component with respect to a fixed axis (z) in space. According to the eigenvalue equation for the Hamiltonian H^0 of the free molecule,

$$H^0 |\gamma JM\rangle = E_{\gamma J} |\gamma JM\rangle, \tag{4}$$

the energy eigenvalues are additionally labelled by γ to specify the levels under consideration (e.g. $+/-$ parity of l-type doublet states or $K_- K_+$ pseudo quantum numbers for energy levels of asymmetric-top molecules).

The total molecular Hamiltonian may be written as

$$H = H^0 - \mu_z \varepsilon \cos \omega t + H^c, \tag{5}$$

where the second term describes the electric dipole interaction of (absorber) molecules with the external microwave radiation, and H^c accounts for intermolecular collisional interaction. μ_z is the electric dipole operator along the electric field component of the plane polarized microwave radiation with amplitude ε and angular frequency ω.

Let us consider radiation-induced transitions between two sets of states $|\gamma_i J_i M\rangle$ and $|\gamma_f J_f M\rangle$, respectively, that are degenerate in absence of external fields and obey the radiative selection rule $\Delta M = 0$. Then,

the relevant equations of motion for off-diagonal and diagonal density matrix elements, respectively, for the system of absorber molecules described here, are given as [14, 15]

$$\dot{\varrho}(iM,fM) = i\omega_0 \varrho(iM, fM) \qquad (6\,a)$$
$$+ i \varkappa_M \varepsilon \cos\omega t [\varrho(fM, fM) - \varrho(iM, iM)]$$
$$- \sum_{M'} \langle\langle iM, fM \mid \Lambda \mid iM', fM' \rangle\rangle \varrho(iM', fM')$$
$$- \sum_{M'} \langle\langle iM, fM \mid \Lambda \mid fM', iM' \rangle\rangle \varrho(fM', iM'),$$

$$\dot{\varrho}(iM, iM) = i \varkappa_M \varepsilon \cos\omega t [\varrho(fM, iM) - \varrho(iM, fM)]$$
$$- \sum_{M'} \langle\langle iM, iM \mid \Lambda \mid iM', iM' \rangle\rangle$$
$$\cdot [\varrho(iM', iM') - \varrho^0(iM', iM')]$$
$$- \sum_{M'} \langle\langle iM, iM \mid \Lambda \mid fM', fM' \rangle\rangle$$
$$\cdot [\varrho(fM', fM') - \varrho^0(fM', fM')] \qquad (6\,b)$$

and corresponding equations for $\varrho(fM, iM)$ and $\varrho(fM, fM)$, where the short notation $|iM\rangle$ and $|fM\rangle$ has been used to specify the states of the considered transition.

The basis functions for the matrix elements in (6a) and (6b) are the eigenfunctions of H^0, and $\omega_0 = (\langle fM | H^0 | fM\rangle - \langle iM | H^0 | iM\rangle)/\hbar$ is the M-independent angular transition frequency. The transition dipole matrix elements are assumed to be real ($\langle iM | \mu_z | fM\rangle = \langle fM | \mu_z | iM\rangle$) and given in units of $\hbar$ by $\varkappa_M$. The effects of molecular collisions due to the contribution of H^c to the Hamiltonian (5) are taken into account by elements of the relaxation supermatrix Λ. In the absence of external radiation, these elements describe first order relaxation to thermal equilibrium, which is assumed to be characterized by a diagonal density matrix and then denoted by ϱ^0. The sums in (6a) and (6b) are extended only over quantum numbers M' of the radiatively connected states of the two-level system, thereby neglecting in particular non-thermal population of all states outside the considered manifold.

No attempt has been made here to consider the effects of translational motion of molecules such as Doppler shift of resonance frequencies, wall collisions and absorber speed dependence of relaxation rates. In addition, with the assumption of a constant electric field amplitude ε of the external microwave radiation, field inhomogeneities due to mode distribution and wall attenuation are not taken into account in the present treatment. The extension to a more general treatment with inclusion of such velocity effects and field inhomogeneities may be given by following earlier theoretical discussions of microwave pulse experiments applied to a system of two non-degenerate energy levels [16, 17].

In general, the above density matrix equations cannot be solved in closed form. Therefore it is instructive to understand the physical behaviour of the M-degenerate two-level system by using approximations. Three cases are considered in the following sections.

III a) Density Matrix Equations in Absence of Collisions

With neglect of relaxation terms, i.e. collisional interaction, the density matrix equations (6a) and (6b) with different M-quantum numbers become decoupled and each M-component of the transition may be treated separately. Then, upon transforming to an interaction representation and making use of the rotating wave approximation, one obtains the following differential equations for each of the M-subsystems in the rotating Feynman-Vernon-Hellwarth (FVH) representation [18]:

$$\dot{U}_M = -\Delta\omega\, V_M, \qquad (7\,a)$$
$$\dot{V}_M = \Delta\omega\, U_M - x_M W_M, \qquad (7\,b)$$
$$\dot{W}_M = x_M V_M\ , \qquad (7\,c)$$

where $\Delta\omega = \omega_0 - \omega$, $x_M = \varkappa_M \varepsilon$, and U_M, V_M, and W_M are the components of a vector $\boldsymbol{r}_M$ in a rotating FVH-space, related to density matrix elements as follows:

$$U_M = \varrho(iM, fM) \exp(-i\omega t)$$
$$+ \varrho(fM, iM) \exp(i\omega t), \qquad (8\,a)$$
$$V_M = i [\varrho(fM, iM) \exp(i\omega t)$$
$$- \varrho(iM, fM) \exp(-i\omega t)], \qquad (8\,b)$$
$$W_M = \varrho(iM, iM) - \varrho(fM, fM). \qquad (8\,c)$$

The above coupled differential equations can be solved by the Laplace transform technique. The solutions are

$$U_M = [x_M^2 U_M(0) + \Delta\omega\, x_M W_M(0)]/\Omega_M^2$$
$$+ ([\Delta\omega^2 U_M(0) - \Delta\omega\, x_M W_M(0)]/\Omega_M^2) \cos\Omega_M t$$
$$- (\Delta\omega\, V_M(0)/\Omega_M) \sin\Omega_M t, \qquad (9\,a)$$
$$V_M = V_M(0) \cos\Omega_M t$$
$$+ ([\Delta\omega\, U_M(0) - x_M W_M(0)]/\Omega_M) \sin\Omega_M t, \qquad (9\,b)$$

$$W_M = [\Delta\omega^2 W_M(0) + \Delta\omega x_M U_M(0)]/\Omega_M^2 + ([x_M^2 W_M(0) - \Delta\omega x_M U_M(0)]/\Omega_M^2)\cos\Omega_M t + (x_M V_M(0)/\Omega_M)\sin\Omega_M t, \quad (9c)$$

where $\boldsymbol{r}_M(0) = (U_M(0), V_M(0), W_M(0))$ is the initial condition of the vector $\boldsymbol{r}_M$ at time $t = 0$, the onset of the external radiation, and $\Omega_M^2 = \Delta\omega^2 + x_M^2$.

Under the resonance condition, $\Delta\omega = 0$, the above solutions can be simplified as

$$U_M = U_M(0), \quad (10a)$$

$$V_M = V_M(0)\cos x_M t - W_M(0)\sin x_M t, \quad (10b)$$

$$W_M = W_M(0)\cos x_M t + V_M(0)\sin x_M t. \quad (10c)$$

The quantities U_M and V_M are related to the macroscopic polarization of the sample, which is the observable quantity in our experiments. Explicitly, the polarization is given by summing over all M-components of the transition [19]:

$$P = N\sum_M \langle iM \mid \mu_z \mid fM\rangle (U_M \cos\omega t - V_M \sin\omega t), \quad (11)$$

where N is the number density of absorber molecules.

With use of a bridge spectrometer driven in the absorption mode, the observed signal is proportional to the polarization component P_1 in quadrature to the external radiation,

$$P_i = N\sum_M \langle iM \mid \mu_z \mid fM\rangle V_M = N\sum_M (-1)^{J_i - M}\begin{pmatrix} J_i & J_f & 1 \\ M & -M & 0\end{pmatrix}\bar{\mu}_{if} V_M, \quad (12)$$

where the Wigner-Eckart theorem has been used, $\bar{\mu}_{if}$ denotes a reduced (M-independent) transition dipole matrix element, and the factor preceding $\bar{\mu}_{if}$ is a $3j$-symbol.

Under the resonance condition, we obtain with (10b), (12) and the definition of x_M

$$P_i = N\sum_M \begin{pmatrix} J_i & J_f & 1 \\ M & -M & 0\end{pmatrix}\bar{\mu}_{if} \cdot\left[(-1)^{J_i - M} V_M(0)\cos\left\{\begin{pmatrix} J_i & J_f & 1 \\ M & -M & 0\end{pmatrix}(\bar{\mu}_{if}\varepsilon/\hbar)t\right\} - W_M(0)\sin\left\{\begin{pmatrix} J_i & J_f & 1 \\ M & -M & 0\end{pmatrix}(\bar{\mu}_{if}\varepsilon/\hbar)t\right\}\right]. \quad (13)$$

The dynamical behaviour of the system under resonant interaction with the external radiation can be described with the solutions (10a–c) or (13) for short pulses, i.e. for pulse lenghts wich are short with respect to the relaxation times characterizing the considered two-level system. However, for M-degenerate energy levels, each M-subsystem is characterizied by its own Rabi angular frequency x_M, and no simple sinusoidal time dependence is generally obtained for P_i to make the concept of $\pi/2$- or π-pulses applicable. Only for special cases such as a roational transition $J = 0-1$, the sum in (13) can be reduced to a single term. For transitions involving higher J-states, P_i exhibits still oscillatory time dependence but the length of "effective $\pi/2$- or π-pulses" may be considerably increased such that the above given solutions of Bloch equations with neglect of relaxation are no longer valid.

This may be seen for example by inspecting the time evolution for P_i of an l-type doublet transition, given with (13) and the initial condition $V_M(0) = 0$ as

$$P_i = -\frac{2NW^0\mu l}{J(J+1)}\sum_{M\geqq 0} M\sin\left\{\frac{Ml}{J(J+1)}(\mu\varepsilon/\hbar)t\right\}, \quad (14)$$

where thermal equilibrium at $t = 0$ has been assumed, i.e. $W_M(0) = W^0$ independent from M,

$$\bar{\mu}_{if} = \mu l\sqrt{(2J+1)/J(J+1)}$$

has been used, and μ is the molecular dipole moment. The sum in (14) is restricted to positive values of M since both $+M$ and $-M$-components of the transition contribute equally to P_i.

In Fig. 1, a plot of $-P_i$, which is proportional to the absorbed MW power [20], vs. $(\mu\varepsilon/h)t$ is shown for two l-type doublet transitions ($l = 1$) with $J = 1$ and $J = 10$, respectively. According to (14) a simple sinusoidal time dependence of P_i is obtained for the $J = 1-1$ transition, giving the length of a (true) π-pulse as $t_\pi = h/\mu\varepsilon$ in this case. The corresponding time for the length of an effective π-pulse for the $J = 10-10$ transition is about 7.5 times longer as indicated on Fig. 1 when P_i is back to zero at $t \approx 7.5\, h/\mu\varepsilon$.

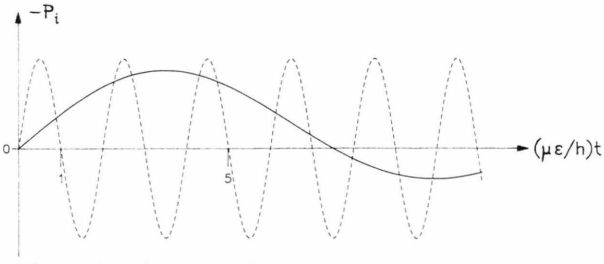

Fig. 1. Plot of $-P_i$ (transient absorption) in arbitrary units vs. $(\mu\varepsilon/h)t$ for l-type doublet transitions ($l = 1$) with $J = 1$ and $J = 10$, respectively. The thermal equilibrium value of the population difference NW^0 is assumed to be identical for both transitions. Dashed line: $J = 1$; continuous line: $J = 10$.

In case of the $J=10-10$ l-type doublet transition of HCN ($l=1$) with $\mu=2.985$ D [21] and a microwave intensity of about 100 mW/cm^2, typical for our experiment, an effective π-condition can then be achieved at $t\approx 0.5$ μs. For the higher pressures used in the experiments (≈ 5 mTorr), this time is comparable to the relaxation times for this transition (≈ 1 μs). The actual pulse length to achieve an effective π-condition is even longer due to microwave field inhomogeneities which are not considered here [17, 22]. Therefore it is then no longer justified to neglect the effects of collisions which are treated in an approximate way in Section IIIc.

IIIb) No External Radiation

With consideration of intermolecular interaction, the relaxation terms in (6a) and (6b) must be included in the theoretical treatment. In the absence of static fields, i.e. M-degenerate rotational energy levels, it is most convenient to expand the density matrix in an irreducible tensorial basis, thereby accounting for its symmetry properties. Explicitly, the following linear combinations of density matrix elements are needed:

$$\varrho_{if}(K,Q)=\sum_{M'M}(-1)^{J_i-M'}(2K+1)^{1/2}\cdot\begin{pmatrix}J_i & J_f & K\\ M' & -M & -Q\end{pmatrix}\varrho(iM',fM). \quad (15)$$

Equation (15) defines so-called "state-multipoles" or "statistical tensors" of rank K and component Q [23]. According to the properties of the $3j$-symbol, K is restricted to integer values between J_i+J_f and $|J_i-J_f|$ (triangular inequality for J_i, J_f and K). Furthermore, for the present case of $\Delta M=0$ spectroscopic selection rules ($M'=M$), only nonthermal elements with $Q=0$ have to be considered, using the short-hand notation $\varrho_{if}(K)$ instead of $\varrho_{if}(K,0)$ in the following. Then, the inverse transformation of (15) is given by

$$\varrho(iM,fM)=\sum_K(-1)^{J_i-M}(2K+1)^{1/2}\begin{pmatrix}J_i & J_f & K\\ M & -M & 0\end{pmatrix}\varrho_{if}(K). \quad (16)$$

In the absence of external radiation, i.e. $\varepsilon=0$ in (6a) and (6b), the time evolution of the system may then be described by differential equations for the state multipoles $\varrho_{if}(K)$ and $\varrho_{ii}(K)$ as follows:

$$\dot{\varrho}_{if}(K)=i\omega_0\varrho_{if}(K)-\Lambda_{ifif}(K)\varrho_{if}(K)-\Lambda_{iffi}(K)\varrho_{fi}(K), \quad (17a)$$

$$\dot{\varrho}_{ii}(K)=-\Lambda_{iiii}(K)[\varrho_{ii}(K)-\varrho^0_{ii}(K)]-\Lambda_{iiff}(K)[\varrho_{ff}(K)-\varrho^0_{ff}(K)] \quad (17b)$$

and corresponding equations for $\varrho_{fi}(K)$ and $\varrho_{ff}(K)$, respectively. The "reduced" relaxation matrix elements $\Lambda_{ifi'f'}(K)$ are independent of Q and describe collisional coupling only between state multipoles of same tensor rank K according to the isotropic nature of the relaxation process. They are related to the Λ-matrix elements by the linear combinations

$$\Lambda_{ifi'f'}(K)=\sum_{M'M}(-1)^{J_i-M'+J_i-M}\begin{pmatrix}J_i & J_f & K\\ M & -M & 0\end{pmatrix}\begin{pmatrix}J'_i & J'_f & K\\ M' & -M' & 0\end{pmatrix}\cdot(2K+1)\langle\!\langle iM,fM|\,\Lambda\,|i'M',f'M'\rangle\!\rangle \quad (18)$$

or the inverse equation

$$\langle\!\langle iM,fM|\,\Lambda\,|i'M',f'M'\rangle\!\rangle=\sum_K(-1)^{J_i-M'+J_i-M}\begin{pmatrix}J_i & J_f & K\\ M & -M & 0\end{pmatrix}\begin{pmatrix}J'_i & J'_f & K\\ M' & -M' & 0\end{pmatrix}\cdot(2K+1)\,\Lambda_{ifi'f'}(K), \quad (19)$$

where K must satisfy simultaneously the triangular inequality for J_i, J_f and J'_i, J'_f, respectively.

We now proceed as in Sect. IIIa by transforming into a rotating FVH-space with introduction of the variables

$$U^K=(-1)^{J_i-J_f}\varrho_{if}(K)\exp(-i\omega t)+\varrho_{fi}(K)\exp(i\omega t), \quad (20a)$$

$$V^K=i[\varrho_{fi}(K)\exp(i\omega t)-(-1)^{J_i-J_f}\varrho_{if}(K)\exp(-i\omega t)], \quad (20b)$$

$$W^K=\varrho_{ii}(K)-\varrho_{ff}(K), \quad (20c)$$

where the definition (20c) of W^K is restricted to integer K-values in the range from 0 to J_l, with J_l being the lower value of J_i and J_f, respectively.

Under the rotating wave approximation, use of (17) and (20) leads to

$$\dot{U}^K=-\Delta\omega V^K-U^K/T_2(K), \quad (21a)$$

$$\dot{V}^K=+\Delta\omega U^K-V^K/T_2(K), \quad (21b)$$

$$\dot{W}^K=-(W^K-W^{K0})/T_1(K), \quad (21c)$$

where

$$1/T_2(K)=\mathrm{Re}\{\Lambda_{ifif}(K)\}, \quad (22a)$$

$$1/T_1(K)=\tfrac{1}{2}\{\Lambda_{iiii}(K)-\Lambda_{iiff}(K)+\Lambda_{ffff}(K)-\Lambda_{ffii}(K)\} \quad (22b)$$

and collision-induced lineshifts have been neglected. W^{K0} is the thermal equilibrium value of W^K, which may be shown with (15) and (20c) to be different from zero only for tensor rank $K=0$.

Equation (21c) has been derived under the assumption of similar scattering dynamics for initial and final states, i.e. $\Lambda_{iiii}(K) + \Lambda_{iiff}(K) \approx \Lambda_{ffff}(K) + \Lambda_{ffii}(K)$ for all K [14]. Extension to more general conditions requires the inclusion of population sums $\varrho_{ii}(K) + \varrho_{ff}(K)$, as treated recently in case of static Stark fields [12].

The Eqs. (21a–c) are solved straightforwardly in case of resonance, $\Delta\omega = 0$, to yield solutions for times $t > 0$ with initial conditions $U^K(0)$, $V^K(0)$ and $W^K(0)$ at $t = 0$:

$$U^K = U^K(0) \exp[-t/T_2(K)], \tag{23a}$$

$$V^K = V^K(0) \exp[-t/T_2(K)], \tag{23b}$$

$$W^K = W^{K0} + (W^K(0) - W^{K0}) \exp[-t/T_1(K)]. \tag{23c}$$

To relate the solutions (23a–c) to the polarization of the sample, only the quantities U_1 and V_1 are needed as seen with use of (11), (12), (15) and (20):

$$P = (N/\sqrt{3})\, \bar{\mu}_{fi} [U^1 \cos \omega t - V^1 \sin \omega t]. \tag{24}$$

Then, the polarization component P_i which is of interest here is given by

$$P_i = (N/\sqrt{3})\, \bar{\mu}_{fi}\, V^1(0) \exp[-t/T_2(1)], \tag{25}$$

independent from the projection quantum number M and describing exponential decay in the absence of radiation.

IIIc) General Case; Approximate Treatment

In the general case, both the effects of external radiation and collisions have to be considered. This may be done either by extending the treatment of Sect. III a with inclusion of relaxation terms, or by adding contributions from radiative interaction to the equations for the state multipoles given in Section III b. In the first case, the density matrix equations with different M-quantum numbers become coupled due to collisional interaction of the molecules. In order to simplify the treatment, it might be tempting to neglect collisional coupling terms with $\Delta M \neq 0$ and thus treat each M-component separately. However, such an approximation would not be very realistic since M-changing and M-preserving collisions are comparable in their contributions to the relaxation process. This may be seen by inspecting the magnitudes of the rate constants for collision-induced transitions from rotational states $|JM\rangle$ to $|J'M'\rangle$, defined by

$$k_{JM,J'M'} = -\langle\langle J'M', J'M' | \Lambda | JM, JM \rangle\rangle, \tag{26}$$

where further state labels γ and γ' have been omitted for simplicity.

For example, the rate constant $K_{JM,00}$, describing collisional population transfer from an arbitrary state $|JM\rangle$ to the rotational ground state $|00\rangle$, is shown to be M-independent with use of (19):

$$k_{JM,00} = (-1)^{J-M-1} \begin{pmatrix} 0 & 0 & 0 \\ 0 & 0 & 0 \end{pmatrix} \begin{pmatrix} J & J & 0 \\ M & -M & 0 \end{pmatrix} \Lambda_{00JJ}(0)$$

$$= -\Lambda_{00JJ}(0)/(2J+1)^{1/2}. \tag{27}$$

Thus, in accordance with the symmetry properties of the relaxation process, it is better to extend the treatment of Sect. III b with inclusion of radiative interaction terms.

General differential equations for the state multipoles $\varrho_{nm}(K)$ ($n, m = i$ or f) can be obtained from the evolution equations (6a, b) with use of (16) and (17) and have been reported previously [15]. For the present case of plane polarized radiation and electric dipole selection rules it then follows that only even K-values ($K = 0, 2, 4, \ldots$) are needed to describe nonthermal population terms $\varrho_{ii}(K)$ and $\varrho_{ff}(k)$, which are denoted in the following shortly as n_i^K and n_f^K, respectively. On the contrary, only odd K-values ($K = 1, 3, 5, \ldots$) characterize the sample coherence through the linear combinations U^K and V^K (20, b) of off-diagonal tensor elements. Due to radiative interaction, tensor elements of rank K are coupled with those of rank $K \pm 1$, e.g. n_i^0 and n_f^0 are coupled to U^1 and V^1, which are in turn coupled to n_i^0, n_f^0, n_i^2 and n_f^2, etc.

In general, the corresponding system of coupled differential equations must be solved numerically. For our purpose to discuss the influence of relaxation in the course of short radiative interaction times it may however be sufficient to use some approximations for simplification of the problem. To do so, we first introduce the average level populations

$$\bar{n}_j = \frac{1}{(2J_j+1)} \sum_M \varrho(jM, jM) \tag{28}$$

with $j = i, f$. Using (15) and the properties of the 3j-symbol, $\bar{n}_j$ may be related to the population-type tensor elements of rank $K = 0$, n_j^0, according to

$$\bar{n}_j = n_j^0/(2J_j+1)^{1/2}. \tag{29}$$

We now proceed by introducing the approximation

$$\bar{n}_j \approx \varrho(jM, jM), \tag{30}$$

which holds strictly only under thermal equilibrium conditions. It then follows with (15) and an orthogonality relation for $3j$-symbols that

$$n_j^K \approx 0 \quad \text{for} \quad K > 0, \tag{31}$$

i.e. all population terms n_i^K and n_f^K with $K = 2, 4, \ldots$ are approximated by the corresponding equilibrium values.

The important consequence of this approximation is the decoupling of the differential equations for state multipoles with $K = 0$ and $K = 1$, namely n_i^0, n_f^0, V^1 and U^1, from all others with higher tensor ranks. Thus, since only V^1 is needed to describe observables in our experiments, the system of differential equations to be considered reduced to

$$\dot{U}^1 = -\Delta\omega\, V^1 - U^1/T_2(1), \tag{32a}$$

$$\dot{V}^1 = \Delta\omega\, U^1 - \bar{x}\{C_{fi}\, n_i^0 - C_{if}\, n_f^0\} - V^1/T_2(1), \tag{32b}$$

$$\dot{n}_i^0 = \bar{x}\, C_{fi}\, V^1/2 + k_{ii}\ \Delta n_i^0 + k_{fi}\, \Delta n_f^0, \tag{32c}$$

$$\dot{n}_f^0 = -\bar{x}\, C_{if}\, V^1/2 + k_{ff}\, \Delta n_f^0 + k_{if}\, \Delta n_i^0, \tag{32d}$$

where

$$C_{fi} = 1/\sqrt{3(2J_i+1)}, \quad C_{if} = 1/\sqrt{3(2J_f+1)},$$

$$\bar{x} = \bar{\mu}_{fi}\, \varepsilon/\hbar,$$

and the deviations of n_i^0 and n_f^0 from thermal equilibrium are denoted by Δn_i^0 and Δn_f^0, respectively. The positive rate constants in (32c) and (32d) are defined by

$$k_{ii} = +\Lambda_{iiii}(0), \tag{33a}$$

$$k_{if} = -\Lambda_{ffii}(0), \tag{33b}$$

and corresponding equations for k_{ff} and k_{fi}, respectively.

In order to derive (32), the general equations as given elsewhere [15] have been used together with approximation (31).

Introducing the variables

$$U = AU^1, \tag{34a}$$

$$V = AV^1, \tag{34b}$$

$$W = (\bar{n}_i - \bar{n}_f) \tag{34c}$$

with $A = \{(J_i + J_f + 1)/(2J_i+1)(2J_f+1)\}^{1/2}$, (32) may be converted with use of (29) into the form of conventional Bloch-type equations for a two-state system [14]:

$$\dot{U} = -\Delta\omega\, V - U/T_2, \tag{35a}$$

$$\dot{V} = \Delta\omega\, U - \tilde{x}\, W - V/T_2, \tag{35b}$$

$$\dot{W} = \tilde{x}\, V - (W - W^0)/T_1, \tag{35c}$$

where $\tilde{x} = A\,\bar{x}/\sqrt{3}$, W^0 is the M-independent thermal equilibrium value of W, and changes of population sum terms $\bar{n}_i + \bar{n}_f$ from equilibrium have been neglected. The relaxation rates (35) are given by

$$1/T_2 = 1/T_2(1) = \mathrm{Re}\,\{\Lambda_{ifif}(1)\}, \tag{36a}$$

$$1/T_1 = \tfrac{1}{2}\{k_{ii} + k_{ff} + k_{if}\, B + k_{fi}/B\}, \tag{36b}$$

where $B = [(2J_i+1)/(2J_f+1)]^{1/2}$, giving $T_1 = T_1(0)$ for Q-branch transitions.

We are interested here in the solutions of (35) for the case of resonance ($\Delta\omega = 0$), which may be obtained by the method of Laplace transforms. With the initial conditions $U(0) = V(0) = 0$ and $W(0) = W^0$ at time $t = 0$, the onset of the radiative interaction, we have for $t < 0$

$$U(t) = 0, \tag{37a}$$

$$V(t) = (W^0/\Omega_p^2)\{\exp(-t/T) \cdot [(\tilde{x}/T_1)\cos\Omega_0 t - (\tilde{x}^3 + \delta\tilde{x}/T_1)\sin\Omega_0 t/\Omega_0] - \tilde{x}/T_1\}, \tag{37b}$$

$$W(t) = (W^0/\Omega_p^2)\{\exp(-t/T) \cdot [\tilde{x}^2\cos\Omega_0 t + (\tilde{x}^2/T)\sin\Omega_0 t/\Omega_0] + 1/(T_1\, T_2)\}, \tag{37c}$$

where

$$1/T = \tfrac{1}{2}(1/T_1 + 1/T_2), \quad \delta = \tfrac{1}{2}(1/T_2 - 1/T_1),$$

$$\Omega_p^2 = 1/(T_1\, T_2) + \tilde{x}^2, \quad \text{and} \quad \Omega_0^2 = \tilde{x}^2 - \delta^2.$$

In most cases of practical interest Ω_0 may be replaced by $\tilde{x}$, the Rabi angular frequency, since it is normally easy to fulfil the conditions $\tilde{x} \gg \delta$. Further simplification may be obtained under the condition of high power and/or low pressure, where the conditions $\tilde{x} \gg 1/T_1$ and $\tilde{x} \gg 1/T_2$ are satisfied. Then, (37) reduces to

$$U(t) = 0, \tag{38a}$$

$$\mathrm{V}\,(\mathrm{t}) = -W^0 \exp(-t/T)\sin\tilde{x}\, t, \tag{38b}$$

$$W(t) = W^0 \exp(-t/T)\cos\tilde{x}\, t, \tag{38c}$$

which account for collisional damping from both T_1- and T_2-relaxation in the exponential terms.

With neglect of contributions from relaxation for sufficiently short times ($t \ll T$), conventional pulse solution as for a two-state system are obtained. In particular, the observable quantity P_i is then given with (24), (34b), and (38b) by

$$P_i = -(NW^0/A\sqrt{3})\,\bar{\mu}_{fi}\sin\tilde{x}\, t. \tag{39}$$

It is interesting to compare the approximate solution (39) for P_i with the exact solution (14) in absence of

collisions given in Sect. III a for the case of a l-type doublet transition. With the definitions of $\bar{\mu}_{fi}$, $\tilde{x}$, and A we then obtain

$$\tilde{P}_i = -\frac{NW^0}{\sqrt{3J(J+1)}}\,\mu\, l(2J+1) \cdot \sin\left\{\frac{l}{\sqrt{3J(J+1)}}(\mu\varepsilon/\hbar)\,t\right\}, \quad (40)$$

where $\tilde{P}_i$ instead of P_i has been introduced here to discriminate from the exact solution (14).

In general $\tilde{P}_i$ is different from P_i. However, for pulse durations which are short with respect to the period of a Rabi oscillation, i.e. $(\mu\varepsilon/\hbar)\,t \ll 1$, we may linearize the time dependence of $\tilde{P}_i$ and P_i, respectively. We then obtain for P_i

$$\tilde{P}_i = -\frac{NW^0}{3J(J+1)}\,\mu\, l^2(2J+1)(\mu\varepsilon/\hbar)\,t\,, \quad (41)$$

and from (14)

$$P_i = -\frac{2NW^0}{J^2(J+1)^2}\,\mu\, l^2(\mu\varepsilon/\hbar)\,t \sum_{M=1}^{J} M^2, \quad (42)$$

which gives the identical result as (41) since $\sum M^2 = J(J+1)(2J+1)/6$. It may also be shown for R- and P-branch transitions with neglect of relaxation that both the rigorous treatment in Sect. III a and the approximate treatment in this section yield identical results for P_i as long as the time dependencies may be linearized for sufficiently short pulses.

With consideration of collisional effects as might be necessary for higher pressures, the two-state Bloch equations (35) are also particularly useful to describe the time evolution of the system for pulse durations which are short with respect to the inverse Rabi frequency.

For longer pulses the corresponding solutions are less accurate, as may be seen for example by comparing the results discussed in Sect. III a for an l-type doublet transition with $l=1$ and $J=1$ or $J=10$, respectively. Using the approximate solution (41) for P_i, the length of a "π-pulse" is given by $t_\pi = \sqrt{3/2}\,(h/\mu\varepsilon) \approx 1.22\,(h/\mu\varepsilon)$ for $J=1$ and $t_\pi \approx 8.80\,(h/\mu\varepsilon)$ for $J=10$. These times are somewhat longer than the previously obtained values for π-pulse periods ($h/\mu\varepsilon$ and $7.5\,(h/\mu\varepsilon)$, respectively) when treating the radiative interaction rigorously.

The above results indicate that the exact treatment of longer pulses requires both the inclusion of relaxation and – due to the radiative interaction – the consideration of tensor terms with $K>1$ in the coupled tensorial Bloch equations, which then must be solved in general numerically. However, as shown in the next section, the treatments in Sects. III a and III b may be used to describe the performed pulse sequence experiments for sufficiently low pressure.

III d) Effect of M-Degeneracy on "π/2"- and "π, τ, π/2"-Pulse Experiments

In a single ("$\pi/2$"-) pulse experiment, the observed signal in the bridge absorption mode is proportional to P_i after pulsed excitation of the molecular sample as described by (25). The effect of M-degeneracy is only contained in the initial conditions at the onset of the transient emission signal. According to the considerations in the previous section, the signal amplitude is depending on the length and amplitude of the microwave pulse and in general also influenced by collisional interactions. However, the decay behaviour of the signal due to relaxation is purely exponential and characterized by a single relaxation time T_2(1). With inclusion of Doppler dephasing [20] we then obtain expression (2), which has been used for data analysis.

For the treatment of the ("π, τ, $\pi/2$"-) pulse sequence experiment we proceed as follows: Assuming sufficiently short pulses, we may neglect collisional effects during the pulse periods and then use the approximate results of Sect. III a for U_M, V_M, and W_M to describe the time evolution of the system. In absence of radiation the time dependencies of U^K, V^K, and W^K are obtained by solving the tensorial Bloch equations according to the treatment in Sect. III b. In order to combine the results from both treatments, it will be necessary to transform from one set of variables into the other. For simplicity we will consider here only Q-branch transitions as applicable to the studied l-type doublet transitions. R- and P-branch transitions are treated similarly, essentially following the same train of thoughts.

For Q-branch transitions we have with (8), (15), (16) and (20)

$$X^K = \sum_M (-1)^{J-M}(2K+1)^{1/2}\begin{pmatrix} J & J & K \\ M & -M & 0 \end{pmatrix} X_M \quad (43)$$

and the inverse equation

$$X_M = \sum_K (-1)^{J-M}(2K+1)^{1/2}\begin{pmatrix} J & J & K \\ M & -M & 0 \end{pmatrix} X^K, \quad (44)$$

where X stands for U, V and W, respectively.

As stated previously, the coherence-type state multipoles U^K and V^K vanish for even values of K, whereas the population-type tensor elements W^K

vanish for odd values of K. In thermal equilibrium, U^K and V^K vanish irrespective of K, and W^K is zero unless $K=0$.

We now identify the times involved in the sequence which starts at $t=0$ with the system in thermal equilibrium conditions ($U_M(0)=V_M(0)$, $W_M(0)=W^0$). After the application of two pulses of length t_1 and t_2, respectively, with a delay time τ between the pulses, the signal is opbserved as a function of τ, taking data after a short delay time τ' with respect to the end of the second pulse.

According to the experimental conditions, only the resonant solutions of the Bloch equations (7) and (21) will be considered. As consequence, the variables U_M as well as U^K remain zero during the sequence and are therefore omitted in the following.

Using (10b, c) and the initial condition at $t=0$, we obtain the following solutions for V_M and W_M at $t=t_1$, the end of the first pulse:

$$V_M(t_1) = -W^0 \sin x_M t_1, \tag{45a}$$

$$W_M(t_1) = W^0 \sin x_M t_1. \tag{45b}$$

In order to describe the system evolution during the delay period between the pulses, we have to use the appropriate treatment of Sect. III b which gives with (23b, c)

$$V^K(t_1+\tau) = V^K(t_1)\exp[-\tau/T_2(K)], \tag{46a}$$

$$W^K(t_1+\tau) = W^{K0}+(W^K(t_1)-W^{K0})\exp[-\tau/T_1(K)], \tag{46b}$$

where the initial conditions $V^K(t_1)$ and $W^K(t_1)$ are obtained with (43) and (45a, b) as

$$V^K(t_1) = -W^0\sum_{M'}(-1)^{J-M'}(2K+1)^{1/2}\cdot\begin{pmatrix} J & J & K \\ M' & -M' & 0\end{pmatrix}\sin x_{M'}t_1 \tag{47a}$$

for odd values of K, and

$$W^K(t_1) = W^0\sum_{M'}(-1)^{J-M'}(2K+1)^{1/2}\cdot\begin{pmatrix} J & J & K \\ M' & -M' & 0\end{pmatrix}\cos x_{M'}t_1 \tag{47b}$$

for even values of K.

The second pulse of length t_2 achieves conversion of population difference to polarization, which is related to the observables in our experiments. Thus, we must consider only the solution for V_M under resonant interaction during the second pulse, which is given with (10b) at time $t=t_1+\tau+t_2$, the end of the pulse, by

$$V_M(t_1+\tau+t_2) = V_M(t_1+\tau)\cos x_M t_2 - W_M(t_1+\tau)\sin x_M t_2. \tag{48}$$

The initial conditions $V_M(t_1+\tau)$ and $W_K(t_1+\tau)$ are given with (44), (46a, b) and (47a, b) by

$$V_M(t_1+\tau) = -W^0\sum_{M'K}R_{MM'K}\exp[-\tau/T_2(K)]\sin x_{M'}t_1, \tag{49a}$$

$$W_M(t_1+\tau) \tag{49b}$$

$$= W^0\sum_{M'K}R_{MM'K}\{1+\exp[-\tau/T_1(K)](\cos x_{M'}t_1-1)\}$$

$$= W^0 + W^0\sum_{M'K}R_{MM'K}\exp[-\tau/T_1(K)](\cos x_{M'}t_1-1),$$

where we have introduced the short notation

$$R_{MM'K} = (-1)^{M-M'}(2K+1)\cdot\begin{pmatrix} J & J & K \\ M & -M & 0\end{pmatrix}\begin{pmatrix} J & J & K \\ M' & -M' & 0\end{pmatrix}, \tag{50}$$

and an orthogonality relation of 3j-symbols ($\sum R_{MM'K}=1$) has been used. According to the properties of V^K and W^K, the sums (49a) and (49b) are restricted to odd and even values of K, respectively.

The transient emission signal which follows the second pulse is proportional to P_i and probed after a short delay time τ' with respect to the pulse end. We therefore need $P_i(t_1+\tau+t_2+\tau')$, which with (25) is given by

$$P_i(t_1+\tau+t_2+\tau') = (N/\sqrt{3})\,\bar{\mu}_{fi}\,V^1(t_1+\tau+t_2)\exp[-\tau'/T_2(1)], \tag{51}$$

where, according to (43) for $K=1$

$$V^1(t_1+\tau+t_2) = \{J(J+1)(2J+1)/3\}^{-1/2}\sum_M M V_M(t_1+\tau+t_2). \tag{52}$$

Since the pulse lengths t_1, t_2 and the delay time τ' remain fixed in the course of one experiment, $P_i(t_1+\tau+t_2+\tau')$ will be denoted shortly as $P_i(\tau)$ in the following and is given with (48), (49a, b), (50), (51) and (52) by

$$P_i(\tau) = D\Big\{\sum_{\substack{K\geq 0\\(\text{even})}}A_K\exp[-\tau/T_1(K)] + \sum_{\substack{K\geq 1\\(\text{odd})}}B_K\exp[-\tau/T_2(K)]+C\Big\}, \tag{53}$$

where

$D(=-NW^0\bar{\mu}_{fi}/\sqrt{J(J+1)(2J+1)}\exp[-\tau'/T_2(1)])$ is independent of τ, and the constants A_K, B_K and C are given by

$$A_K=\sum_{MM'} MR_{MM'K}(\cos x_{M'}t_1-1)\sin x_M t_2, \qquad (54\,a)$$

$$B_K=\sum_{MM'} MR_{MM'K}\sin x_{M'}t_1\cos x_M t_2, \qquad (54\,b)$$

$$C=\sum_M M\sin x_M t_2 \qquad (54\,b)$$

with $A_K=0$ for K odd and $B_K=0$ for K even, respectively.

Both A_K and B_K depend on the lengths t_1 and t_2 of the two pulses, whereas C depends only on the length of the second pulse. With inclusion of Doppler dephasing, which contributes only to the coherence decay terms [17], (53) is of the form of the general expression, (1), for the description of the observed signal in the pulse sequence experiment.

It is interesting to see that, because of M-degeneracy, more information about collision dynamics can generally be obtained in the form of the relaxation parameters $T_1(K)$ (K even) and $T_2(K)$ (K odd) by using a "π, τ, $\pi/2$"-pulse sequence. However, due to the limited accuracy of the experimental results, it was only possible to determine "effecticve" T_1-values for the investigated transitions as described in Section II. This point may be illustrated somewhat more quantitatively with inspection of the theoretical expression for $P_i(\tau)$ for the example of l-type doublet transitions, given with (53) by

$$P_i(\tau)=-\frac{NW^0\mu l}{J(J+1)}\left\{\sum_K A_K\exp[-\tau/T_1(K)\right.$$
$$\left.+\sum_K B_K\exp[-\tau/T_2(K)-\tau^2/4q^2]+C\right\}, \qquad (55)$$

where we have assumed $\tau'=0$ for simplicity and Doppler dephasing has been included in the coherence decay terms.

For $\tau\to\infty$ the sums in (55) vanish and $P_i(\tau\to\infty)$ is then given by solution (14) for single pulse excitation. For finite τ-values, two l-type doublet transitions ($l=1$) with $J=1$ and $J=10$, respectively, may be considered as an example.

According to the discussion in Sect. III a, true π- and $\pi/2$-pulses can be achieved only for the $J=1-1$ transition and are characterized by the lengths $t_1=h/\mu\varepsilon$ and $t_2=h/2\mu\varepsilon$, respectively. Then, using (54 a–c) for the evaluation of A_0 ($=-8/3$), A_2 ($=-4/3$), B_1 ($=0$) and C ($=+2$), we obtain with (55)

$$P_i(\tau)=-NW^0\mu\{1-(4/3)\exp[-\tau/T_1(0)]$$
$$-(2/3)\exp[-\tau/T_1(2)]\}. \qquad (56)$$

Note that $P_i(\tau)\sim 1-2\exp[-\tau/T_1]$ if $T_1(0)=T_2(2)=T_1$ is assumed, which corresponds to the result obtained for two-level systems without M-degeneracy [22] or with $\pm M$-degeneracy in case of static Stark fields [12]. Deviations from single exponential decay behaviour would thus indicate a difference of the two T_1-rates for this transition.

In case of the $J=10-10$ transition, terms up to $K=20$ in (55) must generally be considered. Numerical calculations indicate that the magnitude of the coefficients A_K and B_K decreases rapidly with increasing tensor rank K. For example, choosing $t_1\approx 7.5\,(h/\mu\varepsilon)$ for an effective π-pulse and $t_2\approx 3.5\,(h/\mu\varepsilon)$ for an effective $\pi/2$-pulse, which achieves maximum polarization (see Fig. 1), one obtains $A_K/J(J+1)\approx -1.07$, -0.30, $-0.08,\ldots$ ($K=0, 2, 4, \ldots$) and $B_K/J(J+1)\approx 0$, 0.27, $0.01,\ldots$ ($K=1, 3, 5, \ldots$). Terms with higher K are not quoted since they are too small ($<10^{-3}$) to significantly contribute to the observed signal as described theoretically by (55). This result may be used to justify the asssumptions made for the analysis of the investigated l-type doublet transitions with $J=9$ and $J=10$, respectively, namely the consideration of only one term in the sum for population decay and neglect of all coherence decay terms which are additionally damped due to the Doppler effect.

IV. Results and Discussion

The experimental values for the coefficients β_1 and β_2 to describe the linear pressure dependence of $1/T_1$ and $1/T_2$, respectively, according to (3 a, b) are given in Tables 1 and 2 together with the resonance frequencies for the investigated transitions. Table 1 contains the results for the rotational transition $J=0-1$ of HCCF in the pure gas and for l-type doublet transitions in the (01^10)-state of $HC^{15}N$ with $J=9$ and $J=10$ in the pure gas and mixtures with H_2, D_2 and He. The Table gives also the theoretical values com-

Table 1. Experimental and theoretical values of the coefficients β_1 and β_2 for the linear pressure dependence of $1/T_1$- and $1/T_2$-decay rates for the $J=0-1$ rotational transition of HCCF and two l-type doublet transitions of $HC^{15}N$ at room temperature in the range from 298 K to 303 K. Errors in parantheses are in the last digit given and twice the standard deviation.

System		Transition	Frequency [MHz]	β_1 [μs^{-1} mTorr^{-1}]		β_2 [μs^{-1} mTorr^{-1}]	
Absorber	Perturber			Experiment	Theory	Experiment	Theory
HCCF	HCCF	$J=0-1$	19 412.361	0.0443 (15)	0.0616*	0.0410 (8)	0.0488*
$HC^{15}N$	$HC^{15}N$	l-doublet	19 055.300	0.074 (11)	0.162	0.216 (3)	0.229
	H_2	$J=9$, $v_2=1^1$		0.011 (1)	0.018	0.032 (4)	0.036*
	D_2			0.010 (1)	0.015	0.026 (4)	0.030*
	He			0.009 (2)	0.008	0.012 (1)	0.015*
$HC^{15}N$	$HC^{15}N$	$J=10$, $v_2=1^1$	23 284.616	0.067 (9)	0.162	0.214 (1)	0.227
	H_2			0.012 (2)	0.018	0.033 (5)	0.036*
	D_2			0.010 (1)	0.015	0.025 (5)	0.030*
	He			0.009 (1)	0.008	0.011 (1)	0.015*

* Unnormalized approach [10], others normalized.

Table 2. Experimental and theoretical values of the coefficients β_1 and β_2 for the linear pressure dependence of $1/T_1$- and $1/T_2$-decay rates for different rotational transitions of SO_2 at room temperature in the range from 298 K to 303 K. Errors in parantheses are in the last digit given and twice the standard deviation.

Transition* $J(K_-, K_+) - J'(K'_-, K'_+)$	Frequency [MHz]	β_1 [μs^{-1} mTorr^{-1}]	β_2 [μs^{-1} mTorr^{-1}]	
			This work	Ref. [24]
5(2, 4) – 6(1, 5)	23 414.250	0.0801 (54)	0.0972 (34)	0.0933 (14)
8(2, 6) – 9(1, 9)	24 083.348	0.0870 (40)	0.0966 (28)	0.0969 (10)
12(3, 9) – 13(3, 12)	20 335.405	0.0970 (18)	0.1014 (30)	0.1068 (10)
21(5, 17) – 22(4, 18)	24 039.616	0.0903 (28)	0.1096 (22)	0.1088 (22)
24(4, 20) – 23(5, 19)	22 482.558	0.0907 (40)	0.1062 (46)	0.1082 (24)
35(6, 30) – 34(7, 27)	25 049.443	0.0793 (62)	0.1010 (52)	0.1007 (10)
37(8, 30) – 38(7, 31)	19 637.045	0.0679 (60)	0.0949 (78)	0.0932 (10)

* Upper energy level first.

puted from the theory proposed earlier [10]. Table 2 gives the experimental results for seven rotational transitions of SO_2 in the pure gas. The results for β_2 in this work agree well with previously determined values [24], using a MWFT spectrometer with heterodyne detection of the transient emission signal at an intermediate frequency of about 30 MHz.

According to the discussion in Sect. III, the theoretical values for the pressure dependence of $1/T_1$ and $1/T_2$ may be related to the elements of the relaxation supermatrix Λ. As far as the T_1-rates are concerned, $\beta_1 p$ may then be expressed as a sum over rate constants $k_{jM,j'M'}$ for collision-induced transitions from states $|jM\rangle$ to $|j'M'\rangle$ as defined by (26). Explicitly, using the definition (36 b) of $1/T_1$ and properties of the Λ-matrix [14], we then obtain straightforwardly

$$\beta_1 p = \tfrac{1}{2} \sum_{MM'} \left[\frac{1}{2J_i+1} (k_{iM,fM'} + k_{fM',iM} + \sum_{j \neq i,f} k_{iM,jM'}) + \frac{1}{2J_f+1} (k_{fM,iM'} + k_{iM',fM} + \sum_{j \neq i,f} k_{fM,jM'}) \right]. \quad (57)$$

From the principle of detailed balancing, it follows that $k_{iM,fM'} = k_{fM',iM} \exp(-\hbar\omega_0/kT) \approx k_{fM',iM}$ since the energy level difference for the investigated transitions is small with respect to kT.

Then, (57) may be somewhat simplified to yield a result identical to the expression given elsewhere [25] which was based on a different definition of $1/T_1$. With inspection of (57) we see that there are no contri-

butions to T_1 from pure phase changing collisions since all rate constants describe a change of state. Further there are no contributions to T_1 from reorientation collisions, i.e. collisions of the type $jM \rightarrow jM'$ which change only the projection number M of rotational angular momentum. Finally, comparing the contributions from rates for collision-induced transitions to levels outside the energy levels under consideration ($iM \rightarrow jM'$, $fM \rightarrow jM'$, $j \neq i, f$) with those from rates from population transfer between the two levels ($iM \leftrightarrow fM'$), it follows that the latter contribute approximately with twice the weight. For Q-branch transitions the weight ratio is exactly 2.

Relating the pressure dependence of $1/T_2$ to elements of Λ according to (36 a) leads to a more complicated expression, since it contains contributions from rates for collision-induced level changes, reorientation collisions and state-preserving phase-changing collisions, and the sums over M and M' contain M-dependent weight factors [25]. We will consider here only the result for a $J=0-1$ transition which, identifying the state labels i, f and j only by the rotational quantum numbers 0, 1 and J, respectively, gives [26]

$$\beta_2 p = \tfrac{1}{2}\left(\sum_{J\neq 0,\, M'} k_{00,\,JM'} + \sum_{J\neq 1,\, M'} k_{10,\,JM'}\right) + \tfrac{1}{2}\sum_{M'\neq 0} k_{10,\,1M} + \tfrac{1}{2}(k_{00}+k_{10}), \quad (58)$$

where the last two terms account for "adiabatic" collisions without transfer of energy, characterized by the rate constant

$$k_{01}^{a} = \tfrac{1}{2}\sum_{M'\neq 0} k_{10,\,1M'} + \tfrac{1}{2}(k_{00}+k_{10}). \quad (59)$$

The first sum in (59) describes reorientation collisions within the $J=1$ level, and k_{00} and k_{10} are rate constants to describe collisions which change only the phase of the wave functions for the states $|00\rangle$ and $|10\rangle$, respectively.

Comparing (58) with (57), the difference between the rates $\beta_1 p$ and $\beta_2 p$ is given by

$$\beta_1 p - \beta_2 p = \tfrac{1}{2}\sum_{M'} k_{00,\,1M'} + \tfrac{1}{2} k_{10,\,00} - k_{01}^{a}, \quad (60)$$

i.e. collision-induced transitions between the two levels increase $1/T_1$ whereas adiabatic collisional transitions increase $1/T_2$. The same arguments hold also for transitions involving higher J-states.

As seen from Table 1, the experimental value for β_1 for the $J=0-1$ transition of HCCF is only about 8% larger than the corresponding value for β_2. With regard of the assumptions made in the analysis, e.g. neglect of molecular velocity effects [16, 19] and microwave field inhomogeneities [17], assumption of pure exponential T_1-decay [12], etc., the small difference between the two rates is thought to be not very meaningful. This result of very similar T_1- and T_2-rates has also been found for rotational transitions of linear molecules in low J-states, like OCS [22, 27], HCN [28] and HCCCN [12, 29]. On the contrary, as seen from the further results in Tables 1 and 2, significant differences between the rates for T_1- and T_2-relaxation were found for the investigated systems with HCN and SO_2 as absorber molecules. Except for the HCN – He system, the coefficients β_1 for the pressure dependence of $1/T_1$ are significantly smaller than the corresponding experimental values for β_2. With reference to the present discussion, the observed differences of T_1- and T_2-rates indicate a predominance of adiabatic collision rates which contribute only to $1/T_2$, over the rates for collision-induced transitions between the levels of consideration which contribute more effectively to $1/T_1$.

The results for the J-dependence of β_1 and β_2 for the rotational transitions of SO_2 in Table 2 are illustrated in Fig. 2, indicating an increasing difference between the rates for increasing J. The maximum of the interpolating curves reflects mainly the maximum of the Boltzmann distribution of perturber states, weighting the most effective inelastic collisions with near resonant exchange of rotational energy.

The theoretical results given in Table 1 have been obtained by using the modified Murphy-Boggs theory [30] with consideration of long-range (dipole-, quadrupole-, induction- and dispersion-) intermolecular interaction. For the computation of inelastic rate constants which enter into expression (57) for $1/T_1$, the normalization procedure as proposed earlier [10] has been used except for the results indicated with subscript (*) where the value of N_l is chosen to be 1 in (A 8) of [10]. The molecular parameters for $HC^{15}N$, H_2 and He are given in [10]. The rotational constant for D_2 is given by 917.87 GHz [31], and all other parameters used were the same as for H_2. The parameters used for HCCF were 9.70617 GHz for the rotational constant, 0.75 D for the dipole moment and 7.94 DA for the quadrupole moment as given elsewhere [32].

The observed T_2-rates are generally better reproduced by the theoretical results than the corresponding T_1-rates for which the agreement is in general poor. This indicates the limitations of the exponential

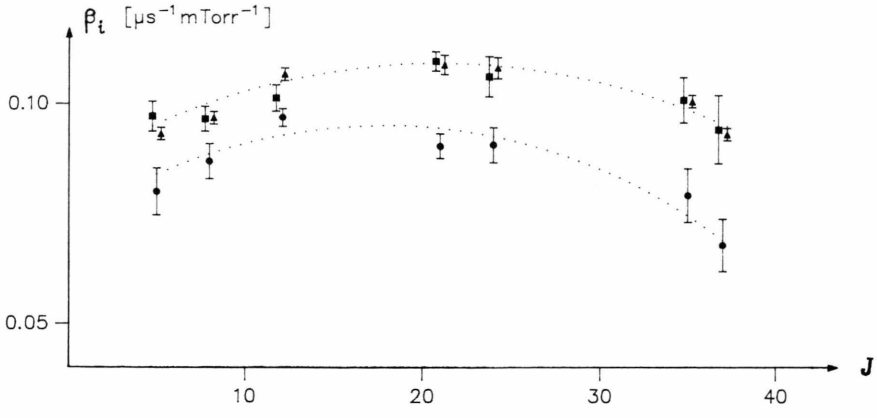

Fig. 2. Experimental values of the coefficients β_i ($i = 1, 2$) for the linear pressure dependence of $1/T_1$ and $1/T_2$ for R- and P-branch rotational transitions of SO_2 vs. rotational quantum number J of upper energy level. Circles: β_1, squares: β_2 (this work), triangles: β_2 (Ref. [24]). Dotted lines: interpolating curves for the J-dependence of β_1 and β_2.

approximation for the non-diagonal matrix elements of the time development operator in [10]. Thus, to understand the observed differences between the T_1- and T_2-rates more quantitatively, a nonperturbative approach or higher order perturbation treatment of collisional scattering dynamics is essential.

V. Conclusion

Summarizing the results of this paper, we conclude that values for the coefficients of the linear pressure dependence of $1/T_1$ and $1/T_2$ have been determined for various molecular systems with transitions in K-band, using a superhet bridge-type spectrometer. For the measurement of both decay rates, identical conditions of pressure and temperature have been used. Except for the $J = 0 - 1$ rotational transition of HCCF, T_1 was found to be significantly greater than T_2 for l-type doublet transitions of $HC^{15}N$ and rotational transitions of SO_2. These results indicate the importance of adiabatic collisions which contribute only to T_2. Such collisions may result from "weak" but also from "strong" collisions, which are not properly treated in the used semiclassical perturbation theory for the binary collision dynamics.

In order to describe the experimental results, a Bloch-type description of the considered two-level systems was used with inclusion of the M-degeneracy of the energy levels. As a consequence, the observable signal in a "π, τ, $\pi/2$"-pulse sequence can be described as a superposition of many exponential terms, giving different information about rotational relaxation. However, because of the limited experimental accuracy and high correlation between the parameters, only one exponential term was used in data analysis to yield an "effective" value for T_1. The values for T_2 were obtained from analysis of transient emission signals which are purely exponential due to collisional interactions.

Acknowledgements

A grant from the Alexander-von-Humboldt-Stiftung to one of us (SCM) and the financial support from the Deutsche Forschungsgemeinschaft and the Fonds der Chemie are gratefully acknowledged. We thank Dr. W. Stahl for critical reading the manuscript. All computations were made at the computer center of Kiel university.

[1] T. G. Schmalz and W. H. Flygare, Laser and Coherence Spectroscopy, p. 125 ff., Plenum Press, New York 1978.
[2] R. H. Schwendeman, Ann. Rev. Phys. Chem. **29,** 537 (1978).
[3] W. E. Hoke, D. R. Bauer, J. Ekkers, and W. H. Flygare, J. Chem. Phys. **64,** 5276 (1976).
[4] T. Amano and R. H. Schwedeman, J. Chem. Phys. **65,** 5133 (1976).
[5] W. E. Hoke, D. R. Bauer, and W. H. Flygare, J. Chem. Phys. **67,** 3454 (1977).
[6] K. Tanaka, J. E. Boggs, and S. C. Mehrotra, Pramana **20,** 439 (1983).
[7] K. L. Peterson and R. H. Schwendeman, J. Chem. Phys. **75,** 5662 (1981).
[8] H. Mäder, W. Lalowski, and R. Schwarz, Z. Naturforsch. **34a,** 1181 (1979).
[9] S. C. Mehrotra and J. E. Boggs, J. Chem. Phys. **62,** 1453 (1975).
[10] S. C. Mehrotra, H. Mäder, J. P. M. de Vreede, and H. A. Dijkerman, Chem. Phys. **93,** 115 (1985).

[11] H. Bomsdorf, H.. Dreizler, and H. Mäder, Z. Naturfosch. **35a,** 723 (1980).
[12] H. Bomsdorf and H. Mäder, Z. Naturforsch. **39a,** 1212 (1984).
[13] H. G. Viehe and E. Franchimont, Chem. Ber. **95,** 319 (1962).
[14] W. K. Liu and R. A. Marcus, J. Chem. Phys. **63,** 272 (1975).
[15] R. H. Schwendeman, J. Chem. Phys. **73,** 4838 (1980).
[16] S. L. Coy, J. Chem. Phys. **73,** 5531 (1980).
[17] H. Mäder, Z. Naturforsch. **34a,** 1170 (1979).
[18] R. P. Feynman, F. L. Vernon jr., and R. W. Hellwarth, J. Appl. Phys. **28,** 49 (1957).
[19] H. Mäder, J. Quant. Spectrosc. Radiat. Transfer **32,** 129 (1984).
[20] J. C. McGurk, T. G. Schmalz, and W. H. Flygare, Adv. Chem. Phys. **25,** 1 (1974).
[21] A. G. Maki, J. Phys. Chem. Ref. Data **3,** 221 (1974).
[22] H. Mäder, J. Ekkers, W. Hoke, and W. H. Flygare, J. Chem. Phys. **62,** 4380 (1974).
[23] K. Blum, Density Matrix. Theory and Applications, p. 85ff., Plenum Press, New York 1981.
[24] S. C. Mehrotra, H. Dreizler, and H. Mäder, Z. Naturforsch. 40a, 683 (1985).
[25] R. H. Schwendeman and T. Amano, J. Chem. Phys. **70,** 962 (1979).
[26] M. J. Burns and S. L. Coy, J. Chem. Phys. **80,** 3544 (1984).
[27] S. L. Coy, J. Chem. Phys. **63,** 5145 (1975).
[28] F. Rohart, Lille (private communication).
[29] S. C. Mehrotra, H. Dreizler, and H. Mäder, J. Quant. Spectrosc. Radiat. Transfer **34,** 229 (1985).
[30] S. C. Mehrotra and J. E. Boggs, J. Chem. Phys. **61,** 5306 (1977).
[31] G. Herzberg, Spectra of Diatomic Molecules, 2nd ed., p. 533, D. van Norstrand, Princeton 1963.
[32] H. Jones and H. D. Rudolph, Z. Naturforsch. **34a,** 340 (1979).